ISSN: 2447-3359

REVISTA DE GEOCIÊNCIAS DO NORDESTE

Northeast Geosciences Journal

v. 12, nº 1 (2026)

https://doi.org/10.21680/2447-3359.2026v12n1ID42195

Assessment of the Positional Accuracy of PPK-Based UAS Orthomosaics and DSM according to PEC-PCD over Steep Slopes

Avaliação da Acurácia posicional de Ortomosaicos e MDS gerados com UAS PPK segundo o PEC-PCD em Encostas Íngremes

Leandro França[1]; Afonso de Paula dos Santos[2]; Ilton Freitas[3]; Sávia Gavazza[4]; Simone Sato[5]

1 Federal University of Pernambuco / Department of Civil Engineering, Recife, PE, Brazil. Email: leandro.franca@ifpb.edu.br
ORCID: https://orcid.org/0000-0003-0863-1926
2 Federal University of Viçosa / Department of Civil Engineering, Viçosa, MG, Brazil. Email: afonso.santos@ufv.br
ORCID: https://orcid.org/0000-0001-7248-4524
3 GeoOne Innovation and Training, João Pessoa/PB, Brazil. Email: ilton@geoone.com.br
ORCID: https://orcid.org/0009-0001-9257-3978
4 Federal University of Pernambuco / Department of Civil Engineering, Recife, PE, Brazil. Email: savia@ufpe.br
ORCID: https://orcid.org/0000-0002-4433-7735
5 Federal University of Pernambuco / Department of Cartographic Engineering, Recife, PE, Brazil. Email: simone.sato@ufpe.br
ORCID: https://orcid.org/0000-0002-2516-8876

Abstract: This study compares the positional accuracy of photogrammetric products: orthomosaic and digital surface model (DSM), generated in a steep slope area in Recife, Brazil, using two UAS platforms: the DJI Mavic 3 Enterprise (M3E) with RTK/PPK and the DJI Mini 3 operating in PPK mode via the T2R solution, with processing performed in both open-source (WebODM/ODM) and proprietary (Agisoft Metashape) environments. The objective was to evaluate horizontal and vertical accuracy without the use of ground control points (GCPs) during processing, employing GCPs exclusively as checkpoints for the computation of positional discrepancies, horizontal, vertical, and three-dimensional RMS, as well as classification according to the Brazilian Cartographic Accuracy Standard for Digital Cartographic Products (PEC-PCD). The processing workflow included rolling shutter correction (for the DJI Mini 3), enforced use of GNSS-derived image coordinates (force-gps) with an adopted accuracy of 0.02 m for camera perspective centers (gps-accuracy), and PPK-corrected geotags obtained via GNSS processing in RTKLib and T2R-Geotagger. Flights were conducted at 100 m altitude (terrain-following), with 85%/75% forward/lateral overlap and a speed of 6 m/s. The results, evaluated in QGIS/LFTools, showed that in Metashape the Mini 3 achieved $RMS_{XY} \approx 9.3$ cm and $RMS_Z \approx 11.5$ cm, while the M3E reached $RMS_{XY} \approx 5.5$ cm and $RMS_Z \approx 4.5$ cm. In WebODM, the Mini 3 achieved $RMS_{XY} \approx 13.1$ cm and $RMS_Z \approx 18.2$ cm, whereas the M3E obtained $RMS_{XY} \approx 6.4$ cm and $RMS_Z \approx 4.8$ cm. Regarding planimetric PEC-PCD classification, the Mini 3 exhibited equivalent performance in both environments — Class B at 1:500 scale and Class A from 1:1,000 onward — while the M3E achieved Class A at all evaluated scales. For vertical PEC-PCD classification, the Mini 3 showed better performance in Metashape (Class B at 1:500 and Class A at 1:1,000), whereas in WebODM a reduction in quality was observed (Class C at 1:500 and Class B at 1:1,000), and the M3E maintained Class A at all scales. It is concluded that the M3E ensures the highest positional accuracy regardless of processing software. However, the Mini 3 operating in PPK demonstrates the capability to produce products compliant with Brazilian cartographic accuracy standards, achieving PEC-PCD Class A up to 1:1,000 in planimetry and up to 1:2,000 in altimetry, representing a lower-cost, high-mobility solution suitable for slope monitoring, infrastructure assessment, and risk management.

Keywords: Positional accuracy; UAS PPK; UAS photogrammetry.

Resumo: Este estudo compara a acurácia posicional de produtos aerofotogramétricos: Ortomosaico e Modelo Digital de Superfície (MDS), gerados em área de encosta íngreme em Recife-PE utilizando dois sistemas UAS: DJI Mavic 3 Enterprise (M3E) com RTK/PPK e DJI Mini 3 operando em PPK via solução T2R, com processamento realizado tanto em ambiente open source (WebODM/ODM) quanto em software proprietário (Agisoft Metashape). O objetivo foi avaliar a acurácia planimétrica e altimétrica sem o uso de pontos de controle no processamento, empregando GCPs exclusivamente como pontos de checagem para cálculo das discrepâncias posicionais, RMS planimétrico, altimétrico e tridimensional, além da classificação conforme o Padrão de Exatidão Cartográfica para Produtos Cartográficos Digitais (PEC-PCD). Nos processamentos aplicaram-se correção de rolling shutter (DJI Mini 3), uso obrigatório das coordenadas precisas das imagens (*force-gps*) com precisão adotada de 0,02 m para os centros perspectivos (*gps-accuracy*) e geotags corrigidas via PPK com processamento GNSS no RTKLib e T2R-Geotagger; os voos seguiram altura de 100 m (*terrain-following*), sobreposição de 85%/75% e velocidade de 6 m/s. Os resultados, avaliados no QGIS/LFTools, mostraram que, no Metashape, o Mini 3 obteve $RMS_{XY} \approx 9,3$ cm e $RMS_Z \approx 11,5$ cm, enquanto o M3E alcançou $RMS_{XY} \approx 5,5$ cm e $RMS_Z \approx 4,5$ cm; já no WebODM, o Mini 3 apresentou $RMS_{XY} \approx 13,1$ cm e $RMS_Z \approx 18,2$ cm, enquanto o M3E obteve $RMS_{XY} \approx 6,4$ cm e $RMS_Z \approx 4,8$ cm. Quanto ao PEC-PCD planimétrico, o Mini 3 apresentou desempenho equivalente nos dois softwares — Classe B para escala 1:500 e Classe A para 1:1.000 e menores — enquanto o M3E alcançou Classe A em todas as escalas; no PEC-PCD altimétrico, o Mini 3 obteve melhor desempenho no Metashape (Classe B em 1:500 e A em 1:1.000), enquanto no WebODM se verificou redução da qualidade (Classe C em 1:500 e B em 1:1.000), e o M3E manteve Classe A em todas as escalas. Conclui-se que o M3E é o UAS que garante maior qualidade posicional independentemente do software, embora o Mini 3 operando em PPK demonstre capacidade de gerar produtos compatíveis com os padrões cartográficos brasileiros, atingindo PEC-PCD Classe A até 1:1.000 na planimetria e até 1:2.000 na altimetria, configurando-se como solução de menor custo, alta mobilidade e aplicabilidade para monitoramento de encostas, infraestrutura e gestão de riscos.

Palavras-chave: Acurácia posicional; UAS PPK; Fotogrametria com UAS.

Received: 22/11/2025; Accepted: 11/03/2026; Published: 31/03/2026.

1. Introduction

The use of drones for geospatial data acquisition has expanded significantly in recent decades, driven by cost reductions, advances in onboard GNSS systems, and improvements in digital photogrammetry algorithms.

In the international scientific context, the term Unmanned Aerial Systems (UAS) is widely adopted due to its comprehensive scope, encompassing not only the aircraft (Unmanned Aerial Vehicle – UAV), but also the control station, communication link, and payloads (COLOMINA; MOLINA, 2014, p. 80). According to Nex et al. (2022, p. 216), UAS represent one of the most significant emerging technologies in geosciences and remote sensing over the past two decades. Although the term "drone" is commonly used in commercial and media contexts, in Brazil the National Civil Aviation Agency (ANAC) and the International Civil Aviation Organization (ICAO) predominantly use the designation Remotely Piloted Aircraft (RPA) in regulatory documents (ANAC, 2017, p. 4). The adoption of the term UAS in this study aims to align with prevailing practices in the international scientific literature, while maintaining terminological correspondence with its equivalents UAV and RPA.

Among the most relevant applications of these platforms, digital photogrammetry stands out, particularly when associated with *Structure from Motion* (SfM) and *Multi-View Stereo* (MVS) techniques, which are capable of generating orthomosaics, dense point clouds, and digital elevation models (DEM) from aerial image datasets (TKÁČ; MÉSÁROŠ, 2019, p. 31). The geometric quality of these products depends on factors such as flight parameters (overlap, altitude, scale), sensor characteristics (focal length, pixel size), block geometry, and the distribution of Ground Control Points (GCPs), as well as effects related to the camera shutter type (ELHADARY et al., 2022, p. 211; MEDEIROS et al., 2025, p. 305; MORA-FELIX et al., 2020, p. 1018).

In sensors with rolling shutter, commonly found in lower-cost CMOS cameras, sequential image capture may introduce distortions, particularly in high-speed flights or over complex terrain; in such cases, acquisition strategies and/or specific rolling shutter modeling can reduce biases (BRUNO; FORLANI, 2023, p. 4; İNCEKARA; SEKER, 2021, p. 550; SIMÕES et al., 2022, p. 347; ZHOU et al., 2020, p. 4). Furthermore, in areas with significant elevation variability, terrain-following flight planning contributes to maintaining a more uniform GSD/scale and, consequently, minimizing distortions and systematic effects (GARGARI et al., 2023, p. 16; GUIMARÃES et al., 2025, p. 44; SINGH; MISHRA; JAIN, 2023, p. 669–670).

Image processing can be carried out using well-established commercial software, such as *Agisoft Metashape* and *Pix4Dmapper*, or through open-source solutions such as *WebODM*, part of the *OpenDroneMap* project (OPENDRONEMAP, 2025, s/p.; TOFFANIN, 2023, p. 3). The latter stands out for its flexibility, algorithm transparency, and lower cost—features inherent to open-source projects, whose code is publicly available for study and reproducibility—making it particularly attractive for educational and research institutions, as well as professionals operating with limited resources (GBAGIR; EK; COLPAERT, 2023, p. 446; KOSTRZEWA et al., 2025, p. 71).

The positional accuracy of photogrammetric products is a central element for the reliability of technical applications, as it directly influences the mapping and monitoring of environmental and urban phenomena (TASCA; FRANCO; SIQUEIRA, 2025, p. 956). Products with high positional accuracy enable detailed analyses of susceptibility to erosional processes, deforestation, uncontrolled urban expansion, degradation of protected areas, monitoring of critical infrastructure, and risks related to flooding and landslides (ARAÚJO SILVA et al., 2025, p. 2055; BRITO et al., 2025, p. 324; PESSOA NETO; LAFAYETTE; CORREA, 2025, p. 14; SILVA et al., 2025, p. 116).

In risk management contexts, such as monitoring mass movements or assessing areas vulnerable to flooding, the availability of high-accuracy mapping derived from lower-cost solutions enables frequent and economically feasible monitoring campaigns, thereby strengthening decision-making processes and supporting the implementation of preventive measures (DO VALE et al., 2025, p. 2877).

To ensure positional quality, image georeferencing can be enhanced using high-precision GNSS receivers through techniques such as *Real-Time Kinematic* (RTK) and *Post-Processed Kinematic* (PPK). In PPK, corrections are applied after the flight using data from a reference station, eliminating the need for real-time correction of image coordinates and allowing the use of precise ephemerides and clock information during post-processing (ARKALI; ATIK, 2025, p. 327).

Regarding the need for ground control, recent studies indicate that PPK can substantially reduce, and in some cases eliminate the dependence on multiple GCPs while maintaining horizontal and vertical accuracy ≤ 10 cm. Nevertheless, when feasible, the use of at least one GCP is recommended to mitigate potential block biases (RAUHALA, 2024, p. 79; TÜRK et al., 2022, p. 476). Additional findings suggest that more robust configurations (e.g., corrections derived from multiple base stations) can further improve vertical accuracy even in the absence of GCPs (MARTÍNEZ-CARRICONDO; AGÜERA-VEGA; CARVAJAL-RAMÍREZ, 2023, p. 4).

In hard-to-access areas, such as steep slopes and unstable terrains, PPK has been successfully applied to produce orthomosaics and elevation models with cartographic-grade quality, reducing operational risks associated with the deployment of GCPs (ŽABOTA; KOBAL, 2021, p. 3–6).

Despite recent advances, a gap remains in the literature regarding the systematic evaluation of the positional accuracy of aerophotogrammetric products obtained with low-cost drones equipped with PPK, such as the DJI Mini 3 integrated with national solutions like the one developed by the T2R company. This gap is particularly relevant because most studies still focus on "Enterprise"-grade UAS with native RTK/PPK capabilities, whereas PPK kits integrated into "entry"-level platforms have strong potential to democratize high-precision mapping.

The lack of evidence becomes even more evident when simultaneous validation of orthomosaics and digital elevation models (DEM) is required, based on absolute three-dimensional coordinates obtained from high-precision GNSS as reference, especially in challenging contexts such as steep slopes and highly variable terrain.

This study aims to address this gap by providing an original assessment of the performance of the Mini 3 UAS operating in PPK mode, processed in WebODM for surveys over steep slopes, considering both horizontal and vertical accuracy metrics. In this context, the following hypothesis is proposed: entry-level UAS, such as the DJI Mini 3 equipped with PPK, can produce orthomosaics and digital elevation models (DEM) with sufficient quality for engineering and environmental monitoring applications, even in high-slope areas, provided that appropriate flight planning (high overlap, terrain-following) and quality control procedures are adopted.

The main objective of this study is to evaluate whether low-cost drones, such as the Mini 3 operating in PPK mode, can replace, under certain processing conditions, enterprise-grade solutions, such as the Mavic 3E, in slope surveys without the use of ground control points, while maintaining compliance with positional accuracy standards established by current norms and specifications.

Specifically, the study aims to: (1) quantify the impact of these choices on horizontal and vertical accuracy through discrepancies in X, Y, and Z, RMS (XY/Z), and PEC-PCD classification, using high-precision GNSS coordinates as reference; and (2) compare the performance of the Mini 3 PPK with that of a higher-end platform (Mavic 3E, RTK/PPK), as well as across processing environments using open-source software (WebODM) and commercial software (Agisoft Metashape) under equivalent conditions.

2. Methodology

2.1 Study Area

The study area is located in the Morro Alto do Reservatório region, in Recife, Pernambuco, Brazil, covering approximately 0.4 km². Figure 1 presents the study area, along with the spatial distribution of the checkpoints used for positional accuracy assessment.

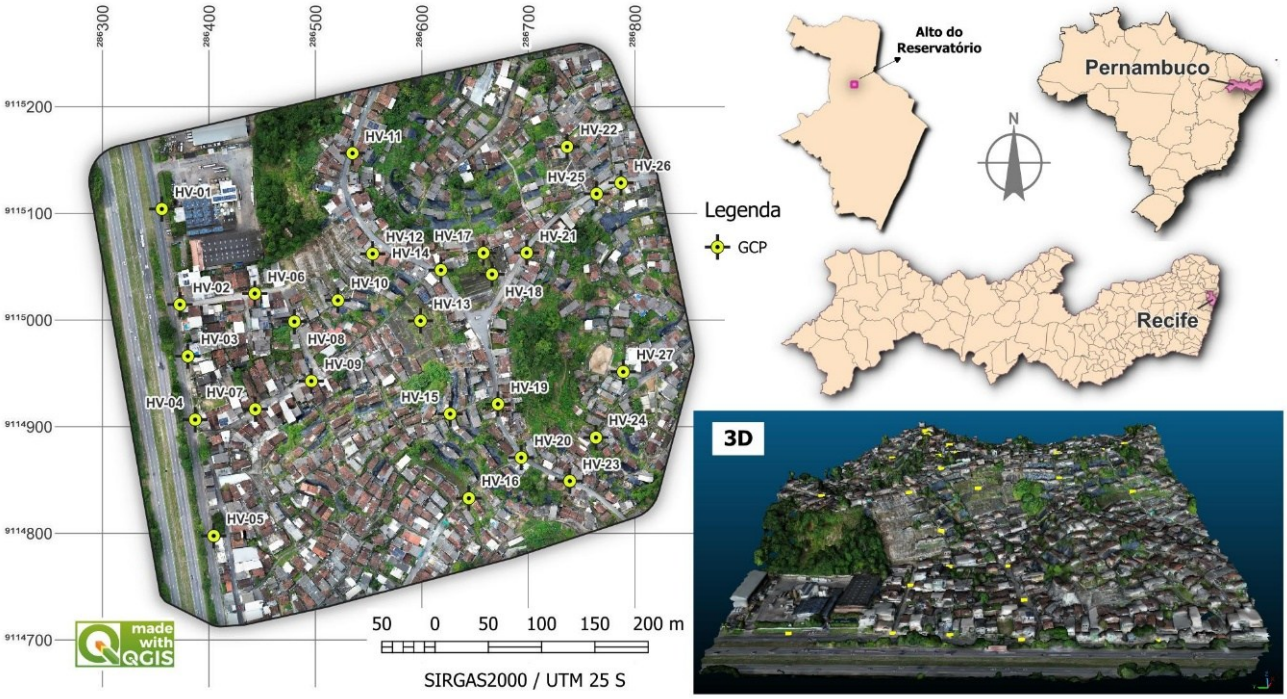

Figure 1 – Location map of the study area at Morro Alto do Reservatório, Recife–PE, Brazil.
Source: Authors (2025).

2.2 Equipment, Software, and Versions

The equipment and software used in this study were as follows:

- Aircraft: DJI Mini 3 (with T2R PPK kit) and DJI Mavic 3E (RTK/PPK).
- GNSS: Polaris S100 geodetic receiver (L1/L2).
- Flight planning and mission execution: QGIS 3.40.9 with the GeoFlight Planner plugin (planning), and mission execution via the Litchi Pilot application.
- Photogrammetric processing (open source): WebODM 2.8.1 with OpenDroneMap engine 3.5.5.
- Photogrammetric processing (commercial): Agisoft Metashape 2.2.0 (with parameters aligned to those used in WebODM) for comparison between processing software.
- PPK and geotagging: RTKLib (demo5 b34d) for post-processing and T2R Geotagger v1.0.63 for writing corrected coordinates into image metadata.
- Quality assessment: QGIS 3.40.9 with LFTools v2.4.0 for computing discrepancies in X, Y, and Z, planimetric and vertical RMS, and classification according to the Cartographic Accuracy Standard (PEC-PCD).

2.3 Flight Planning

Flights were planned in QGIS (GeoFlight Planner plugin) with 85% forward overlap, 75% lateral overlap, 100 m AGL, and a flight speed of 6 m/s. Here, AGL (Above Ground Level) denotes the height relative to the terrain beneath each waypoint, rather than the takeoff point.

The missions were exported and executed in Litchi Pilot app, with altitude defined in the Mission Hub using the Above Ground mode (terrain following), in which waypoint altitudes are calculated relative to the ground based on online elevation data integrated into Litchi (the provider/DEM is not publicly disclosed). For an operational reference of this mode and its limitations, see the Litchi Mission Utilities documentation on "Above Ground" (LITCHI UTILITIES, n.d., n.p.).

2.4 Ground Control

The GCPs used as checkpoints were surveyed using a Polaris S100 geodetic GNSS receiver through the Fast Static relative positioning method: 5 minutes of observation at the rover for each point, with a base station tracking for more than 4 hours and coordinates corrected via static relative positioning using a RBMC station in Recife–PE. All raw data were converted to RINEX format and processed in RTKLib. The final coordinates were used as absolute reference for validating the photogrammetric products (orthomosaics and DEM).

2.5 UAS PPK Processing

The PPK processing of the UAS data was performed using RTKLib (demo5 b34d), generating a refined trajectory of the aircraft. Subsequently, T2R Geotagger (v1.0.63) was used to write the corrected time-position coordinates into the EXIF metadata of the images captured by the Mini 3 UAS (and the Mavic 3E, also operated in PPK mode), ensuring precise temporal alignment between the camera at the moment of image capture and the GNSS solution.

2.6 Photogrammetric Processing in WebODM

The main processing was conducted in WebODM using the *High Resolution* preset with the parameter *pc-quality = High*, aiming to maximize point cloud densification, feature definition, and the overall quality of orthomosaics and elevation models (OPENDRONEMAP, 2025). This configuration was kept constant across all scenarios to ensure direct comparability of results and to isolate the effects of the evaluated factors.

The accuracy analysis was based on the following methodological assumptions: (i) mandatory use of GNSS-derived image coordinates with a priori accuracy defined by *gps-accuracy* associated with the *force-gps* parameter set to 2 cm, and (ii) application of rolling shutter correction.

Methodological justifications:

- Use of PPK: Post-processed correction of image geotags enables more accurate estimation of camera perspective center coordinates, resulting in SfM models and photogrammetric products that are better aligned with the actual terrain, thereby reducing the dependence on ground control points for block georeferencing.
- Rolling shutter correction: Enabling this feature mitigates geometric distortions caused by the sequential readout typical of CMOS sensors, particularly along the flight direction, improving internal block consistency and the geometric fidelity of mapped features.
- "Force-gps" parameter and "gps-accuracy" definition: The assignment of appropriate weights to GNSS observations is a critical factor in the adjustment process. Overly optimistic values (e.g., 0.02 m) may impose excessive rigidity on the block, forcing the incorporation of systematic errors from the geotags; whereas overly permissive weights (e.g., 1 m) reduce the influence of the PPK solution and degrade positional accuracy. The choice of 2 cm represents a methodological compromise based on flight stability, camera performance, and the consistency of the fixed PPK solution.

2.7 Photogrammetric Processing in Agisoft Metashape

To isolate the effect of the processing software while maintaining methodological consistency with WebODM, PPK-geotagged images (RTKLib + T2R Geotagger) were imported into Agisoft Metashape, adopting the same weighting criteria for the geotags. In *Reference Settings*, the parameter *Camera location accuracy* was set to 0.02 m (for both XY and Z), equivalent to the optimal configuration in WebODM (*force-gps* + *gps-accuracy* = 0.02 m). Rolling shutter correction was enabled for the DJI Mini 3 and not applied to the Mavic 3E (mechanical shutter). Image alignment was performed at high quality with reference preselection (using PPK-derived positions), followed by *Optimize Cameras*, weighting GNSS observations according to the defined accuracy (Agisoft, 2025).

During reconstruction, *Depth Maps* and the *Dense Cloud* were generated at high quality; the DSM was derived from the dense point cloud, and the orthomosaic was produced while maintaining a GSD consistent with the flight parameters (100 m altitude, terrain-following).

2.8 Positional Quality Assessment

In the comparative experiments, 26 independent checkpoints (with no GCPs used during processing), surveyed using GNSS, were employed to ensure direct comparability between processing platforms (WebODM × Metashape) and UAS (Mini 3 × Mavic 3E). For each point, discrepancies in the X, Y, and Z components were computed as the differences between the values

derived from the photogrammetric products and the geodetic reference values obtained using a geodetic GNSS receiver (with accuracy better than 1 cm in 3D).

For planimetric products (orthomosaics), target centers were measured directly on the raster; for the vertical component, elevations were extracted from the digital surface model (DSM). This approach follows the concept of absolute positional accuracy adopted in standards and technical guidelines (BRASIL, 2016, p. 3–21; ISO, 2023, p. 1; ASPRS, 2024, p. 17).

The evaluation was performed in QGIS 3.40.9 using the LFTools 2.4.0 plugin, computing positional discrepancies, horizontal RMS (XY) and vertical RMS (Z), as well as classification according to the PEC-PCD standard.

Statistical Formulation

According to França et al. (2019), the accuracy measure proposed by Gauss is the Mean Square Error (MSE), in which σ^2 represents the variance (random component) and b represents the trend (systematic component), also known as bias.

$$MSE = \frac{\sum_{i=1}^{N} \varepsilon_i^2}{N} \simeq \sigma^2 + b^2 \tag{1}$$

The error (ε) is defined as the difference between the observed value and the true value. Since the true value is not directly observable, the concept of discrepancy (d) is used, defined as:

$$d = v_t - v_r \tag{2}$$

Where $v_t$is the test value of the X, Y, or Z component obtained from the photogrammetric products, and $v_r$is the reference value of the corresponding point derived from the geodetic GNSS survey.

The bias (mean) and precision (standard deviation) of the discrepancies are given by:

$$b = \frac{\sum_{i=1}^{N} d_i}{N} \tag{3}$$

$$\sigma = \sqrt{\frac{\sum_{i=1}^{N} (d_i - \bar{d})^2}{N}} \tag{4}$$

Accuracy is expressed by the RMS value, i.e., the square root of the MSE:

$$RMS = \sqrt{\frac{\sum_{i=1}^{N} {d_i}^2}{N}} \tag{5}$$

For each component, it can be expressed as:

- $RMS_X = \sqrt{\frac{\sum_{i=1}^{N} {dX_i}^2}{N}}$
- $RMS_Y = \sqrt{\frac{\sum_{i=1}^{N} {dY_i}^2}{N}}$
- $RMS_Z = \sqrt{\frac{\sum_{i=1}^{N} {dZ_i}^2}{N}}$

The planimetric RMS_{XY} is given by:

$$RMS_{XY} = \sqrt{{RMS_X}^2 + {RMS_Y}^2} \tag{6}$$

PEC-PCD classification was derived from the discrepancies (d) and RMS values obtained, following the specifications of ET-CQDG (BRASIL, 2016), with Maximum Error (ME) and Standard Error (SE) values defined in Table 1.

Table 1 — PEC-PCD and PEC standards, in meters, for large-scale mapping.

Tipo	PEC-PCD	PEC	1:500	1:1,000	1:2,000	1:5,000	1:10,000

	(2016)	*(1984)*	**EM**	**EP**	**EM**	**EP**	**EM**	**EP**	**EM**	**EP**	**EM**	**EP**
Planimetria	**A**	**-**	0.14	0.085	0.28	0.17	0.56	0.34	1.40	0.85	2.80	1.70
	B	**A**	0.25	0.15	0.50	0.30	1.00	0.60	2.50	1.50	5.00	3.00
	C	**B**	0.40	0.25	0.80	0.50	1.60	1.00	4.00	2.50	8.00	5.00
	D	**C**	0.50	0.30	1.00	0.60	2.00	1.20	5.00	3.00	10.00	6.00
Altimetria	**A**	**-**	0.135	0.085	0.27	0.17	0.27	0.17	0.54	0.34	1.35	0.84
	B	**A**	0.25	0.165	0.50	0.33	0.50	0.33	1.00	0.67	2.50	1.67
	C	**B**	0.30	0.20	0.60	0.40	0.60	0.40	1.20	0.80	3.00	2.00
	D	**C**	0.375	0.25	0.75	0.50	0.75	0.50	1.50	1.00	3.75	2.50

Source: Adapted from ET-CQDG (BRASIL, 2016, p. 4–9).

3. Results and Discussion

For the evaluation of positional accuracy, 26 independent checkpoints were used. The images acquired by the DJI Mini 3 and DJI Mavic 3E (M3E) UAS were processed using PPK-corrected geotags, without the use of GCPs, in both WebODM/OpenDroneMap and Agisoft Metashape, adopting equivalent processing parameters, as described in Section 2.

3.1 Evaluation of Planimetric Positional Accuracy (XY)

Table 2 presents the statistics of discrepancies dX, dY, and dXY, considering the processing results obtained from the tested software for both UAS platforms.

To facilitate the spatial interpretation of planimetric uncertainties, Figure 2 presents the error ellipses derived from the Variance–Covariance Matrix (VCM) at a 68% confidence level, corresponding to dispersion within one standard deviation. This representation provides a consistent visualization of the planimetric distribution of discrepancies dX and dY between test points and their respective reference coordinates.

The size and orientation of the ellipses simultaneously express the magnitude and anisotropy of uncertainty: larger ellipses indicate greater variance and, consequently, lower precision, while the major axis reveals the direction of maximum dispersion (CARVALHO et al., 2024, p. 494). Bias is interpreted from the displacement of the ellipse center relative to the origin ($dX = 0$, $dY = 0$); the smaller this displacement, the lower the systematic effect, whereas significant offsets indicate potential residual biases.

Table 2 – Statistics of discrepancies in the dX, dY, and dXY components for products generated by WebODM and Agisoft Metashape, using the Mini 3 and M3E UAS.

Component	**Statistics of discrepancies**	**WebODM / OpenDroneMap**		**Agisoft Metashape**	
		Mini 3	**Mavic 3E**	**Mini 3**	**Mavic 3E**
$\mathbf{d_X}$	Máx. (m)	0.154	0.055	0.121	0.058
	Min. (m)	-0.229	-0.110	-0.104	-0.170
	Média (m)	-0.015	-0.027	0.004	-0.015
	Desvio-padrão (m)	0.071	0.040	0.051	0.042
	RMS (m)	0.072	0.048	0.052	0.045
$\mathbf{d_Y}$	Máx. (m)	0.309	0.130	0.229	0.128
	Min. (m)	-0.223	-0.089	-0.145	-0.023
	Média (m)	0.020	0.003	0.009	0.010
	Desvio-padrão (m)	0.107	0.043	0.077	0.031
	RMS (m)	0.109	0.044	0.079	0.033
$\mathbf{d_{XY}}$	Máx. (m)	0.385	0.170	0.252	0.213
	Min. (m)	0.021	0.007	0.029	0.007
	Média (m)	0.105	0.056	0.078	0.039
	Desvio-padrão (m)	0.079	0.032	0.051	0.040

	RMS (m)	**0.131**	**0.064**	**0.093**	**0.055**

Source: Authors (2025).

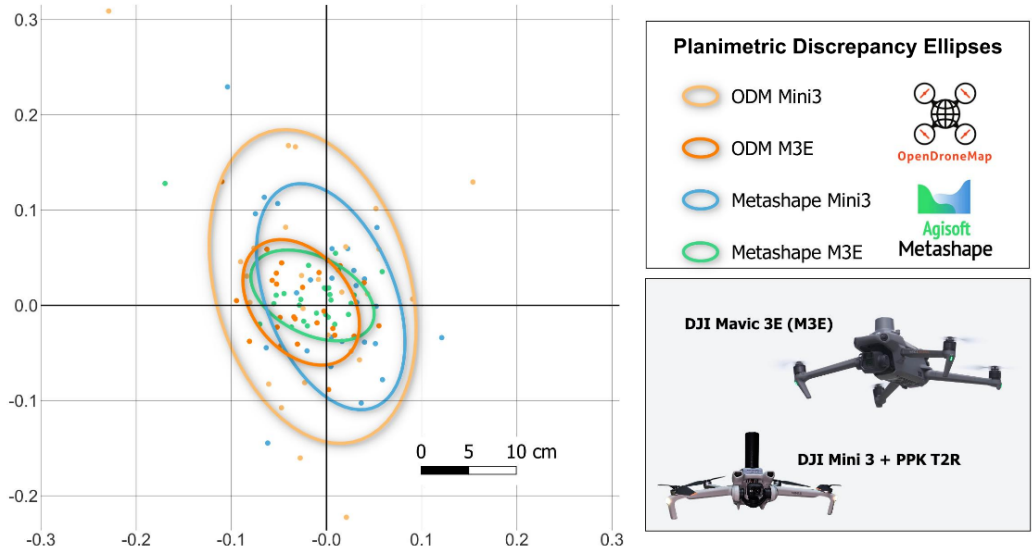

Figure 2 – Ellipses of planimetric discrepancies from the processing results.
Source: Authors (2025).

The two largest ellipses represent the distribution of uncertainties associated with the DJI Mini 3, indicating broader discrepancies; the results from Metashape showed a better concentration of residuals around (0,0) when compared to WebODM. The two smaller ellipses correspond to the results of the DJI Mavic 3E (M3E), which demonstrated, in both software environments, precise and accurate results, with RMSXY < 6.4 cm (Table 4).

The M3E combines a 4/3" CMOS sensor with a mechanical shutter (1/2000 s), significantly reducing motion blur and rolling shutter effects, thereby improving mapping precision. In contrast, the Mini 3 features a 1/1.3" CMOS sensor and an electronic shutter (rolling shutter), requiring specific correction during processing and remaining more susceptible to slight motion blur. Additionally, the estimated spatial resolutions at 100 m were 3.48 cm (Mini 3) and 2.67 cm (M3E), which may have contributed to more accurate identification of target centers and stronger block geometry in the M3E. In summary, camera characteristics and GSD directly influence overall positional accuracy.

As shown in Table 6, the M3E achieved an RMSXY approximately two times lower than that of the Mini 3. Nevertheless, the Mini 3 operating with PPK (without GCPs) achieved RMSXY values of 9 cm in Metashape and 13 cm in WebODM, demonstrating its viability for engineering applications that do not require very high positional accuracy.

Evaluation of Vertical Positional Accuracy (Z)

The quality of the vertical component (Z) is essential for studies in steep terrain and slope monitoring. The vertical accuracy of the DEMs was assessed based on discrepancies dZ between elevations extracted from the tested products and the reference high-precision GNSS coordinates.

In Table 3, the following metrics were adopted: mean (bias), standard deviation (precision), and RMSZ (overall indicator of vertical accuracy), allowing the distinction between trend, dispersion, and accuracy. This evaluation is particularly important because uncertainties in Z tend to be amplified in rugged terrain, potentially compromising geomorphological analyses, volume calculations, and stability assessments.

Table 3 – Statistics of vertical discrepancies and RMS_Z

Software	**UAS**	**Altimetric discrepancies (in meters)**				
		Máx	**Min**	**Média**	**Desvio Padrão**	**RMS_Z**
WebODM / OpenDroneMap	Mini 3	0.427	0.021	0.159	0.088	**0.182**
	Mavic 3E	0.042	-0.114	-0.032	0.037	**0.048**
Agisoft Metashape	Mini 3	0.214	-0.043	0.100	0.058	**0.115**

	Mavic 3E	0.085	-0.054	0.027	0.036	**0.045**

Source: Authors (2025).

Figure 3 presents boxplots of the vertical discrepancies (dZ) calculated between homologous points (test and reference), with elevations extracted from the DSM and planimetric identification performed on the orthomosaic, combining the results from both software environments (WebODM and Metashape) and the two analyzed UAS (DJI Mini 3 and Mavic 3E).

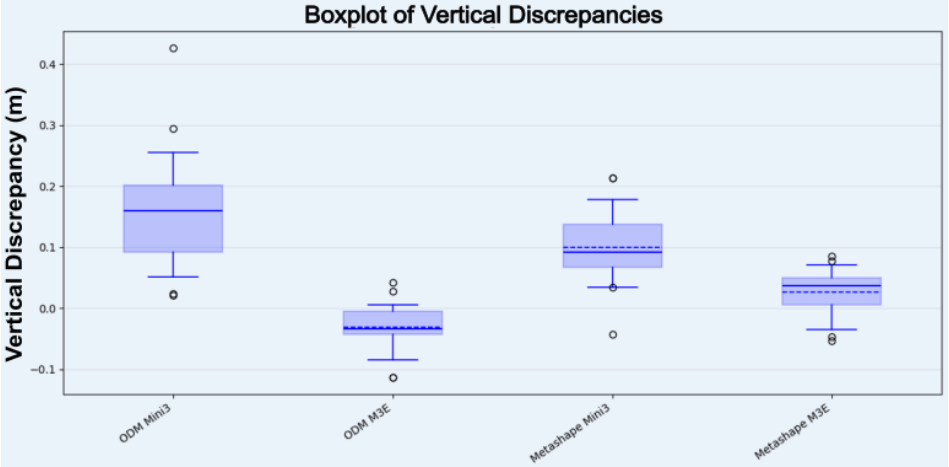

Figure 3 – Boxplot of the analyzed vertical discrepancies.
Source: Authors (2025).

From Figure 3, it can be observed that the largest vertical discrepancies occur in the Mini 3 processing using WebODM, with a higher number of outliers. In the other cases, discrepancies are concentrated near zero, with particular emphasis on the Mavic 3E, whose bias (mean) is below 3.2 cm, as shown in Table 3.

3.2 Classification According to Decree 89.817 / ET-CQDG

Regarding the Cartographic Accuracy Standard for Digital Cartographic Products (PEC-PCD), Tables 4 and 5 present the quality classification (horizontal and vertical) for the main cadastral mapping scales. For both drones and processing software, the results were consistent with the Brazilian positional accuracy requirements established in national technical specifications.

Table 4 – Planimetric PEC-PCD.

Software	**UAS**	**Planimetric Cartographic Accuracy Standard**				
		1:500	**1:1,000**	**1:2,000**	**1:5,000**	**1:10,000**
WebODM / OpenDroneMap	Mini 3	B	A	A	A	A
	Mavic 3E	A	A	A	A	A
Agisoft Metashape	Mini 3	B	A	A	A	A
	Mavic 3E	A	A	A	A	A

Source: Authors (2025).

Table 5 – Vertical PEC-PCD.

Software	**UAS**	**Vertical Cartographic Accuracy Standard**				
		1:500	**1:1,000**	**1:2,000**	**1:5,000**	**1:10,000**
WebODM / OpenDroneMap	Mini 3	C	B	B	A	A
	Mavic 3E	A	A	A	A	A
Agisoft Metashape	Mini 3	B	A	A	A	A
	Mavic 3E	A	A	A	A	A

Source: Authors (2025).

4. Final Considerations

The comparison between platforms and processing environments showed that the Mavic 3E (larger sensor and mechanical shutter) achieved lower RMS values and more stable PEC-PCD classifications, particularly due to reduced vertical variability. Nevertheless, the Mini 3 operating in PPK mode achieved standards compatible with technical applications, for example, PEC-PCD Class A up to 1:1,000 (XY) and Class A up to 1:2,000 (Z), confirming its viability as a low-cost solution for frequent monitoring of slopes, infrastructure, and environmental processes. In disaster and humanitarian response scenarios, the open and accessible processing chain (RTKLib + T2R Geotagger + WebODM/QGIS) enables rapid deployment, local collaboration, and cost reduction, enhancing temporal update capacity and supporting decision-making.

As a methodological delimitation and opportunity for further research, this study focused on a single steep-slope area, with fixed flight parameters (altitude/overlap/speed) and high-resolution presets in WebODM. While these choices favor reproducibility in both field acquisition and processing, they limit generalization, requiring further investigation in different areas and processing conditions. Therefore, future work should include: (i) sensitivity analysis of *gps-accuracy* (including cross-flight configurations and alternative weighting of GNSS observations); (ii) stratification by slope, land use, and vegetation cover to investigate spatial error patterns; (iii) experiments with varying flight heights, camera angles, speeds, and overlap, explicitly evaluating the impact of rolling shutter; (iv) exploration of advanced ODM/Metashape parameters to reduce vertical biases; (v) interpretation and spatial analysis of discrepancies (anisotropies, doming/tilting) and their relationship with block geometry and terrain; and (vi) evaluation of terrain-following approaches using different DEM sources. These guidelines tend to reduce reliance on GCPs and maximize accuracy when applying PPK in more accessible UAS platforms, reinforcing the method's potential for applications in risk-prone areas and disaster management.

Acknowledgements

The authors would like to thank T2R for providing the Mini 3 PPK drone used in this research. The authors also acknowledge the support of the Department of Cartographic Engineering at the Federal University of Pernambuco (UFPE) for providing the Mavic 3E drone. Field support from students of the Graduate Program in Geodetic Sciences and Geoinformation Technologies (PPGCGTG) and the Graduate Program in Civil Engineering (PPGEC), both at UFPE, is also gratefully acknowledged. Finally, the authors thank the reviewers for their valuable comments and contributions, which helped improve this work.

References

AGISOFT. *Aerial data processing (without GCPs)*. 2025. Disponível em: https://agisoft.freshdesk.com/support/solutions/articles/31000157908-aerial-data-processing-without-gcps-. Acesso em: 18 ago. 2025.

AMERICAN SOCIETY FOR PHOTOGRAMMETRY AND REMOTE SENSING (ASPRS). *ASPRS Positional Accuracy Standards for Digital Geospatial Data*. Edition 2, Version 2. 2024. https://doi.org/10.14358/ASPRS.PAS.2024.

ANAC. *Regulamento Brasileiro da Aviação Civil Especial – RBAC-E nº 94: Regras gerais para aeronaves não tripuladas de uso civil*. Agência Nacional de Aviação Civil, 2017. Disponível em: https://www.gov.br/defesa/pt-br/arquivos/ajuste-01/cartografia/divcar/2020/05-rbac-e-94_anac_rpa-vant_02_05_2017.pdf . Acesso em: 11 ago. 2025.

ARAÚJO SILVA, Emanuel et al. Uso de Aeronave Remotamente Pilotada para Extração de Variáveis Dendrométricas de uma Floresta Tropical Seca. *Revista Brasileira de Geografia Física*, *[S. l.]*, v. 18, n. 3, p. 2054–2068, 2025. DOI: https://doi.org/10.26848/rbgf.v18.3.p2054-2068.

ARKALI, Mehmet; ATIK, Muhammed Enes. Accuracy Assessment of RTK, PPK, and PPP-AR Techniques for Direct Georeferencing in UAV-Based Photogrammetric Mapping. *The International Archives of the Photogrammetry, Remote Sensing and Spatial Information Sciences*, v. 48, p. 325-330, 2025. DOI: https://doi.org/10.5194/isprs-archives-XLVIII-M-6-2025-325-2025.

BRASIL. Exército Brasileiro. Diretoria de Serviço Geográfico. *Norma da Especificação Técnica para Controle de Qualidade de Dados Geoespaciais (ET-CQDG).* EB80-N-72.004. 1. ed. Brasília, 2016.

BRITO, Edmundo Rodrigues de; BASTOS, Frederico de Holanda; CORDEIRO, Abner Monteiro Nunes; SILVA, Ícaro Breno da; PAULA, Davis Pereira de; CARVALHO, Rodrigo Guimarães de; SOARES, Hildebrando dos Santos. Modelagem hidráulica aplicada à análise de riscos de inundação em áreas urbanas brasileiras: o caso da Zona Especial de Interesse Social (ZEIS) do Lagamar, Fortaleza (Nordeste do Brasil). *Caminhos de Geografia*, Uberlândia, v. 26, n. 103, p. 320–340, 2025. DOI: 10.14393/RCG2610375334.

BRUNO, Nazarena; FORLANI, Gianfranco. Experimental tests and simulations on correction models for the rolling shutter effect in UAV photogrammetry. *Remote Sensing*, v. 15, n. 9, p. 2391, 2023. DOI: https://doi.org/10.3390/rs15092391.

CARVALHO, V. A.; SANTOS, A. de P. dos; CUNHA, M. M.; BARBOSA, L. da S.; DAL POZ, W. R.; MEDEIROS, N. das G.; OLIVEIRA, J. C. de. Aplicação da estatística direcional no controle de qualidade cartográfica. *Revista de Geociências do Nordeste*, v. 10, n. 2, p. 491–503, 2024. DOI: 10.21680/2447-3359.2024v10n2ID36253. Disponível em: https://periodicos.ufrn.br/revistadoregne/article/view/36253. Acesso em: 6 fev. 2026.

COLOMINA, I.; MOLINA, P. Unmanned aerial systems for photogrammetry and remote sensing: A review. *ISPRS Journal of Photogrammetry and Remote Sensing*, v. 92, p. 79-97, jun. 2014. DOI: https://doi.org/10.1016/j.isprsjprs.2014.02.013.

MEDEIROS, L. Í. B., GRAÇA, A. J. S., FAGGION, P. L., VEIGA, L. A. K. Análise comparativa da flexão de barra metálica sob cargas, por diferentes métodos geodésicos: nivelamento geométrico, nivelamento trigonométrico e fotogrametria a curtas distâncias. *Revista de Geociências do Nordeste*, v.11, n.1, p.299-313, 2025. DOI: https://doi.org/10.21680/2447-3359.2025v11n1ID36387.

DO VALE, Leonardo; CASADO, Alberto; FERNANDES, Bruno; COSTA, Glauber; HUMBERTO AQUINO ROCHA, Joaquin. Monitoramento de Pontes e Viadutos com Uso de Veículo Aereo Não Tripulado (Vant): Estudos de Caso. *Revista Brasileira de Geografia Física*, *[S. l.]*, v. 18, n. 4, p. 2864–2881, 2025. DOI: https://doi.org/10.26848/rbgf.v18.4.p2864-2881.

ELHADARY, A.; RABAH, M.; GHANIM, E.; MOHIE, R.; TAHA, A. The influence of flight height and overlap on UAV imagery over featureless surfaces and constructing formulas predicting the geometrical accuracy. NRIAG *Journal of Astronomy and Geophysics*, v. 11, n. 1, p. 210-223, 2022. DOI: https://doi.org/10.1080/20909977.2022.2057148.

FRANÇA, L. L. S.; PENHA, A. L. T.; CARVALHO, J. A. B. Comparison between absolute and relative positional accuracy assessment-a case study applied to digital elevation models. *Boletim de Ciências Geodésicas*, v. 25, p. e2019003, 2019. DOI: http://dx.doi.org/10.1590/s1982-21702019000100003.

FRANCO, Guilherme Gandra; NAIME, André Fonseca. Structure From Motion (SfM)–Uma breve revisão histórica, aplicações nas geociências e perspectivas futuras. *Anuário do Instituto de Geociências*, v. 44, 2021. DOI: https://doi.org/10.11137/1982-3908_2021_44_40853.

GARGARI, A. M.; EBADI, H.; ESMAEILI, F.; LATIFZADEH, S. Dynamic 3D network design for UAV-based photogrammetry in mountainous terrain. Environmental *Earth Sciences*, v. 82, n. 7, p. 188, 2023. DOI: https://doi.org/10.1007/s12665-023-10864-9.

GBAGIR, Augustine-Moses Gaavwase; EK, Kylli; COLPAERT, Alfred. OpenDroneMap: multi-platform performance analysis. *Geographies*, v. 3, n. 3, p. 446-458, 2023. DOI: https://doi.org/10.3390/geographies3030023.

GUIMARÃES, M. J. M., DA SILVA SANTOS, A. C., DA SILVA, A. S., RIBEIRO, D. P., BARROS, J. R. A., & LOPES, I. Mapeamento topográfico com aeronave remotamente pilotada para fins de georreferenciamento de propriedades rurais: Topographic mapping with remotely piloted aircraft for georeferencing rural properties. *Revista de Geociências do Nordeste*, v. 11, n. 1, p. 42-57, 2025. DOI: https://doi.org/10.21680/2447-3359.2025v11n1ID34481.

İNCEKARA, Abdullah Harun; SEKER, Dursun Zafer. Rolling shutter effect on the accuracy of photogrammetric product produced by low-cost UAV. *International Journal of Environment and Geoinformatics*, v. 8, n. 4, p. 549-553, 2021. DOI: https://doi.org/10.30897/ijegeo.948676.

INTERNATIONAL ORGANIZATION FOR STANDARDIZATION. *Geographic information — Data quality — Part 1: General requirements*. ISO 19157-1:2023. Geneva: ISO, 2023.

KANAI, S. A review of structure-from-motion and multi-view-stereo. *J. of the Japan Society of Photogrammetry and Remote Sensing*, v. 60, n. 3, p. 95-99, 2021. DOI: https://doi.org/10.4287/jsprs.60.95.

KOSTRZEWA, A., PŁATEK-ŻAK, A., BANAT, P., & WILK, Ł. Open-Source vs. Commercial Photogrammetry: Comparing Accuracy and Efficiency of OpenDroneMap and Agisoft Metashape. *The International Archives of the Photogrammetry, Remote Sensing and Spatial Information Sciences*, v. 48, p. 65-72, 2025. DOI: https://doi.org/10.5194/isprs-archives-XLVIII-1-W4-2025-65-2025.

LITCHI UTILITIES. *How Does Litchi's "Above Ground" Option Work. s.d.* Disponível em: https://www.litchiutilities.com/docs/aboveGround.php. Acesso em: 6 fev. 2026.

MARTÍNEZ-CARRICONDO, Patricio; AGÜERA-VEGA, Francisco; CARVAJAL-RAMÍREZ, Fernando. Accuracy assessment of RTK/PPK UAV-photogrammetry projects using differential corrections from multiple GNSS fixed base stations. *Geocarto International*, v. 38, n. 1, p. 2197507, 2023. DOI: https://doi.org/10.1080/10106049.2023.2197507.

MORA-FELIX, Zuriel Dathan et al. Effect of photogrammetric RPAS flight parameters on plani-altimetric accuracy of DTM. *Open Geosciences*, v. 12, n. 1, p. 1017-1035, 2020. DOI: https://doi.org/10.1515/geo-2020-0189.

NEX, F., ARMENAKIS, C., CRAMER, M., CUCCI, D. A., GERKE, M., HONKAVAARA, E. & SKALOUD, J. UAV in the advent of the twenties: Where we stand and what is next. *ISPRS Journal of Photogrammetry and Remote Sensing*, v. 184, p. 215–242, 2022. DOI: https://doi.org/10.1016/j.isprsjprs.2021.12.006.

OPENDRONEMAP COMMUNITY. OpenDroneMap (ODM) v3.5.5: *Open Source Toolkit for Processing Aerial Imagery* [software]. 2025. Disponível em: https://github.com/OpenDroneMap/ODM e https://www.opendronemap.org. Acesso em: 11 ago. 2025.

PESSOA NETO, A. G.; LAFAYETTE, K. P. V.; CORREA, M. M. Mapeamento de suscetibilidade a processos erosivos na bacia hidrográfica do rio Tejipió/PE. *Caminhos de Geografia*, Uberlândia, v. 26, n. 103, p. 13–28, 2025. DOI: 10.14393/RCG2610372785.

RAUHALA, A. Accuracy assessment of UAS photogrammetry with GCP and PPK-assisted georeferencing. *In: International conference on FinDrones*. Cham: Springer Nature Switzerland, 2023. p. 57-73. DOI: https://link.springer.com/chapter/10.1007/978-3-031-44607-8_4.

SIMÕES, D. P., DE OLIVEIRA, H. C., JÚNIOR, O. F. L., & COSTA, D. C. Métodos de Planejamento de Rotas para RPAs: uma Revisão da Literatura. *Rev. Bras. Cartogr*, v. 74, n. 2, 2022. DOI: http://dx.doi.org/10.14393/rbcv74n2-60138.

SILVA, M. A. S.; RODRIGUES, M. M.; ARNAUT, L. R.; LACERDA, H. C.; SILVA, M. G. C.; SOARES, W. O.; FARIA, A. L. L.. Análise de áreas de preservação permanente de curso hídrico em Viçosa (MG) por meio de imagens de aeronave remotamente pilotada. *Caminhos de Geografia*, Uberlândia, v. 26, n. 105, p. 111–129, 2025. DOI: 10.14393/RCG2610575643.

SINGH, Chandra Has; MISHRA, Vishal; JAIN, Kamal. High-resolution mapping of forested hills using real-time UAV terrain following. *ISPRS Annals of the Photogrammetry, Remote Sensing and Spatial Information Sciences*, v. 10, p. 665-671, 2023. DOI: https://doi.org/10.5194/isprs-annals-X-1-W1-2023-665-2023.

TASCA, B. F. C.; FRANCO, F. M.; SIQUEIRA, A. J. B. Remotely Piloted Aircraft Systems (RPAS): a fast and accurate way for monitoring landfills: Remotely Piloted Aircraft Systems (RPAS): a fast and accurate way for monitoring landfills. *Revista de Geociências do Nordeste*, v. 11, n. 1, p. 955-969, 2025. DOI: https://doi.org/10.21680/2447-3359.2025v11n1ID39327.

TKÁČ, Matúš; MÉSÁROŠ, Peter. Utilizing drone technology in the civil engineering. *Journal of Civil Engineering*, v. 14, n. 1, p. 27-37, 2019. DOI: https://doi.org/10.1515/sspjce-2019-0003.

TOFFANIN, Piero. *OpenDroneMap: The Missing Guide: A Practical Guide to Drone Mapping Using Free and Open Source Software.* 2. ed. UAV4GEO, 2023.

TÜRK, Tarık et al. Accuracy assessment of UAV-post-processing kinematic (PPK) and UAV-traditional (with ground control points) georeferencing methods. *Environmental Monitoring and Assessment*, v. 194, n. 7, p. 476, 2022. DOI: https://link.springer.com/article/10.1007/s10661-022-10170-0.

WANG, Tao; GAN, Vincent JL. Enhancing 3D reconstruction of textureless indoor scenes with IndoReal multi-view stereo (MVS). *Automation in Construction*, v. 166, p. 105600, 2024. DOI: https://doi.org/10.1016/j.autcon.2024.105600.

ŽABOTA, B.; KOBAL, M. Accuracy assessment of uav-photogrammetric-derived products using PPK and GCPs in challenging terrains: In search of optimized rockfall mapping. *Remote Sensing*, v. 13, n. 19, p. 3812, 2021. DOI: https://doi.org/10.3390/rs13193812.

ZHOU, Yilin et al. A two-step approach for the correction of rolling shutter distortion in UAV photogrammetry. ISPRS Journal of Photogrammetry and Remote Sensing, v. 160, p. 51–66, fev. 2020. DOI: https://doi.org/10.1016/j.isprsjprs.2019.11.020.